

Response to Associate Editor's comments:

Interactive comment on "Inferring the effects of sink strength on plant carbon balance processes from experimental measurements" by Mahmud et al.

Associate Editor Decision: Publish subject to minor revisions (review by editor) (04 Jun 2018) by Sönke Zaehle

Response to Associate Editor:

Overall Review

Many thanks for your revised manuscript, which does satisfactorily address all concerns raised by the reviewers. Based on my own reading of the revised manuscript, I have a small range of minor, editorial suggestions to help improve the clarity of the manuscript. Looking forward to receiving a final version of the manuscript in short time.

We appreciate the Associate Editor's comments and careful reading of our manuscript.

Minor editorial comments:

L 56: is the "and" necessary here? In my view the implementation in models is solely discussed because of the multiple roles NCSs are assumed to play in plants.

The "and" is now removed (line 56).

L110-113. I would avoid mixing hypotheses and the justification of your approach here. Maybe having these added sentences after the added sentence in L107, and then continuing "Therefore, we tested ... " would be clearer?

The sentences are reorganised as suggested (line 110-116).

L209: Am I to deduce from this that you assume that the tissue-specific dark respiration rate of leaves rate of used to estimate maintenance respiration rates also for woody and root tissues? What's the justification for this simplification?

This assumption is based on work by Drake et al. (2017) showing tissue-specific dark respiration rates of different organs are similar in *Eucalyptus tereticornis* seedlings. We have added this reference in the text (line 206-209).

eq 7: Does not use a_r . This makes it inconsistent with the text in 223-227 and the figure 1. Why not use a_r in the equation, but add to caption and L223-227 that a_r is defined as $1 - a_{w,r}$. This would avoid introducing an inline equation (which should be avoided) in line 247

All these are adjusted according to the comment (eq 7, line 226, 233, 254).

L231 (eq 8-10): Probably hair-splitting, but actually these equations should read

$C_{t,f} = k_{n,f} * C_n + C_{s,f}$, etc

for consistency with eq 4-7 and you probably should repeat the partitioning now mentioned in L178.

The equations are modified according to the suggestion (eq 8-10, line 235).

L443: I think that the use of the term “one at a time” is misleading here, because this term strictly means keeping all other parameters at their standard values (corresponding to your individual scheme). From reading this text, I would assume that Figure 5 shows exactly what happens if each parameter is change once to “free” while all the others are kept at 5L, which is not what you’ve done nor what figure 5 shows.

The confusion is now clarified in line 451.

L444-5: I wonder if this would be clearer if you stated explicitly that you change from the parameter set derived from DA on the 5L observations to that of the parameters obtained when using the free seedlings as constraint of the model? Please design and label table 4 such that it is not necessary to refer to “columns” of the Table in the text.

The text (line 459-462) and the table are refined.

L453: This sentence reads repetitive from the preceding ones. Please make sure that the newly added text is better integrated

The paragraph is reorganised and the problem of repetition is now resolved.

L448 remove (+/-)

Removed from line 454.

L448: rather remove “both”, and add “, respectively” in the end?

Modified (line 454-455).

L563: add “in seedlings”.

Added in line 575.

Figure 3 caption. remind the reader that ar is implied from af and aw, for instance by putting this explicit in the Yaxis label. Simply to avoid the reader assuming you have 6 free parameters-

Figure 3 caption and Y-axis label are modified.

Table 1: Be more explicit to state “leaf area feedback on photosynthesis and Rm”?

Stated explicitly.

Table 1: Simset C better “5L and free seedlings treatment considered”

Altered.

Table 1: I am not sure that “parameters changes one at a time” describes what you do here when you change an increasing number of parameters from the DA result of 5L to free

Corrected.

Figure 4 caption: Add “Simulated” (or similar) to the beginning of the first sentence. Assuming this is what is shown. Remove duplicate bracket in “Container size (L)”

Amended.

Figure 5 caption: I am unsure about the term “input” parameters, as these plots describe the prescribed change in model parameters, but they are not really the “input”, which are temperature and ?

Changed to “inferred” parameters.

Figure 5 caption: Please reminder the reader that you are sequentially changing the parameter values from 5L to free.

Repeated the simulation scenario in figure caption.

Figure 5 caption: I think this figure would be much easier to follow if panels A-F used always the same colours for 5L and free. The link between the colours in A-F and G-I is not evident, certainly not for daltonians.

The colours of the panels A-F are now adapted having the same colours for 5 L and free seedlings in all 6 panels.

SI: Unclear what “optimum” parameter settings are. Do you mean the DA posterior?

Yes, indeed. The text is now clarified in S1 figure caption.

1 **Inferring the effects of sink strength on plant carbon balance processes from**
2 **experimental measurements**

3 Kashif Mahmud¹, Belinda E. Medlyn¹, Remko A. Duursma¹, Courtney Company^{1,2}, Martin
4 G. De Kauwe³

5

6 ¹Hawkesbury Institute for the Environment, Western Sydney University, Locked Bag 1797,
7 Penrith NSW 2751, Australia

8 ²Department of Biology, Colgate University, NY 13346, USA

9 ³ARC Centre of Excellence for Climate Extremes, University of New South Wales, Sydney,
10 NSW 2052, Australia

11 *Correspondence to:* Kashif Mahmud (k.mahmud@westernsydney.edu.au)

12

13 **Abstract**

14 The lack of correlation between photosynthesis and plant growth under sink-limited
15 conditions is a long-standing puzzle in plant ecophysiology that currently severely
16 compromises our models of vegetation responses to global change. To address this puzzle,
17 we applied data assimilation to an experiment where sink strength of *Eucalyptus tereticornis*
18 seedlings were manipulated by restricting root volume. Our goals were to infer which
19 processes were affected by sink limitation, and to attribute the overall reduction in growth
20 observed in the experiment, to the effects on various carbon (C) component processes. Our
21 analysis was able to infer that, in addition to a reduction in photosynthetic rates, sink
22 limitation reduced the rate of utilization of non-structural carbohydrate (NSC), enhanced
23 respiratory losses, modified C allocation and increased foliage turnover. Each of these effects
24 was found to have a significant impact on final plant biomass accumulation. We also found
25 that inclusion of a NSC storage pool was necessary to capture seedling growth over time,
26 particularly for sink limited seedlings. Our approach of applying data assimilation to infer C
27 balance processes in a manipulative experiment enabled us to extract new information on the
28 timing, magnitude, and direction of the internal C fluxes from an existing dataset. We suggest

29 this approach could, if used more widely, be an invaluable tool to develop appropriate
30 representations of sink-limited growth in terrestrial biosphere models.

31

32 **Keywords:** Non-structural carbohydrate, carbon allocation, data assimilation, mass-balance,
33 photosynthesis, plant growth, sink regulation

34

35 **1 Introduction**

36 Almost all mechanistic models of terrestrial vegetation function are based on the carbon (C)
37 balance: plant growth is represented as the difference between C uptake (through
38 photosynthesis) and C loss (through respiration and turnover of plant parts). This approach to
39 modeling plant growth dates back to early crop and forest production models (McMurtrie and
40 Wolf, 1983; de Wit and van Keulen, 1987; de Wit, 1978) and now provides the fundamental
41 quantitative framework to integrate our scientific understanding of plant ecosystem function
42 (Makela et al., 2000).

43 However, C balance models have been criticized for being “source-focused” (Fatichi et al.,
44 2014). Most C balance models predict growth from the environmental responses of
45 photosynthesis (“source limitation”). In contrast to this assumption, many experimental
46 studies demonstrate that growth is directly limited by environmental conditions (“sink
47 limitation”) rather than the availability of photosynthate. For example, growth is more
48 sensitive to water limitation than is photosynthesis (Bradford and Hsiao, 1982; Müller et al.,
49 2011; Mitchell et al., 2014); low temperatures are considerably more limiting to cell division
50 than to photosynthesis (Körner et al., 2014); nutrient limitation may slow growth without
51 reducing photosynthesis (Reich, 2012; Crous and Ellsworth, 2004); and, physical sink-
52 limitation may reduce growth with a decline in photosynthetic capacity and an accumulation
53 of leaf starch (Arp, 1991; Campany et al., 2017; Poorter et al., 2012a; Paul and Foyer, 2001).

54 How can we move to models that include both source- and sink-limitation? There is ongoing
55 discussion about realistic implementations of non-structural carbohydrates (NSC) in
56 vegetation **models because** of their multiple roles in plant functioning, such an
57 implementation provides a buffer against discrepancies in source and sink activity. Some C

58 balance models include a “storage” pool of NSC (Running and Gower, 1991; Bossel, 1996;
59 Thornley and Cannell, 2000), but most of these models make the assumption that the NSC
60 pool acts merely as a buffer between C sources and sinks, balancing out seasonally or at least
61 over several seasons (Fatichi et al., 2014; Friend et al., 2014; De Kauwe et al., 2014; Schiestl-
62 Aalto et al., 2015). There is mounting evidence that the NSC plays a more active role in tree
63 physiology (Buckley, 2005; Sala et al., 2012; Wiley and Helliker, 2012; Hartmann et al.,
64 2015). For example, NSC accumulation can lead to down-regulation of photosynthesis
65 (Nikinmaa et al., 2014). Therefore, the need to quantify the NSC pool and to better
66 understand the prioritisation of storage vs. growth is of great importance.

67 An understanding of the dynamics of storage is also essential to correctly represent the C
68 balance in models (Hartmann and Trumbore, 2016). If, for example, a direct growth
69 limitation is implemented into models, how should the surplus of accumulated photosynthates
70 be treated? In their proof-of-concept sink-limited model, Fatichi et al. (2014) allowed
71 reserves to accumulate indefinitely. Alternatively, some models (e.g. CABLE (Law et al.,
72 2006), O-CN (Zaehle and Friend, 2010)) increase respiration rates when excess labile C
73 accumulates. Both approaches can be seen as model-oriented solutions to maintain C balance
74 that are unsatisfactory because they are not based on empirical data. Experiments where sink
75 strength is manipulated may provide the key to improve our understanding of C balance
76 processes under direct growth limitation.

77 Efforts have been made to understand the physiological and morphological changes in
78 response to belowground C sink limitation by manipulating rooting volume in tree seedlings
79 (Arp, 1991; Company et al., 2017; Poorter et al., 2012a). These experiments often reveal
80 photosynthetic down-regulation and accumulation of leaf starch, and reductions in growth
81 (Arp, 1991; McConnaughay and Bazzaz, 1991; Gunderson and Wullschleger, 1994; Sage,
82 1994; Poorter et al., 2012a; Robbins and Pharr, 1988; Maina et al., 2002; Company et al.,
83 2017). In a recent study with Eucalyptus seedlings, Company et al. (2017) showed that the
84 reduction in seedling growth when rooting volume was restricted could not be completely
85 explained by the negative effects of sink limitation on photosynthesis, suggesting that other
86 components of the C balance were affected in the process. However, Company et al. (2017)
87 could not accurately quantify all components of tree C balance, i.e. photosynthesis,
88 carbohydrate storage, biomass partitioning and respiration.

89 Quantifying all components of C balance is not an easy task, given that not all processes are
90 measured with equal fidelity, and data gaps will always occur. Klein and Hoch (2015) used a
91 C mass balance approach with a tabular process flowchart to decipher C components and
92 provide a full description of tree C allocation dynamics. Here, rather than using a manual
93 process, we used a data assimilation (DA)-modelling framework, which has been proven to
94 be a powerful tool in analyzing complex C balance problems (Williams et al., 2005;
95 Richardson et al., 2013). For example, Richardson et al. (2013) use DA to discriminate
96 among alternative models for the dynamics of non-structural carbon (NSC), finding that a
97 model with two NSC pools, fast and slow, performed best; Rowland et al. (2014) applied DA
98 to experimental observations of ecosystem C stocks and fluxes to infer seasonal shifts in C
99 allocation and plant respiration in an Amazon forest; and Bloom et al. (2016) used DA to
100 constrain a C balance model with satellite-derived measurements of leaf C, to simulate
101 continental-scale patterns in C cycle processes.

102 Our goal in this paper was to use DA to quantify the impact of sink limitation on C balance
103 processes. We utilized data from an experiment in which sink limitation was induced by
104 restricting the rooting volume of *Eucalyptus tereticornis* seedlings over the course of 4
105 months (Campany et al., 2017). We assimilated photosynthesis and growth measurements
106 from the experiment into a simple C balance model, to infer the effects of sink limitation on
107 the main C balance processes, namely: respiration, carbohydrate utilization, allocation, and
108 turnover.

109 Although in reality plants do have a storage component, it is not necessarily the case that
110 including such a storage component in the model leads to model improvement. Hence, it is
111 important to test whether or not adding the storage component improves the performance of
112 the model enough to justify the additional complexity. Therefore, we first tested two null
113 hypotheses:

114 H1: There is no need to consider storage in the model: growth can be adequately predicted
115 from current day photosynthate.

116 H2: There is no effect of sink limitation on C balance processes other than via a reduction of
117 photosynthesis.

118 We were then interested to test the following specific hypotheses about the impact of sink
119 limitation on C balance:

120 H3: We hypothesized that the rate of utilization of carbohydrate for plant growth would be
121 lower under sink limitation, causing growth rates to slow and non-structural carbohydrate to
122 accumulate.

123 H4: We hypothesized that under sink limitation a larger proportion of C would be lost to
124 growth respiration and less used for production. We have dubbed this the “wasteful plant”
125 hypothesis; this hypothesis corresponds to the assumption embedded in some models that
126 respiration is up-regulated when labile C accumulates e.g. CABLE, O-CN (Law et al., 2006;
127 Zaehle and Friend, 2010).

128 H5: We hypothesized that foliage and root C allocation fractions would be reduced, in favour
129 of wood allocation. Sink limitation induced by nutrient and/or water stress often results in a
130 shift in C allocation away from foliage and towards fine roots (Poorter et al., 2012b).
131 However, for this experiment, the physical restriction of root growth limits the potential for
132 root allocation. Hence, we predicted that both foliage and fine root allocation would decrease.
133

134 **2 Materials and Methods**

135 **2.1 Experiment description**

136 The site and experimental setup have been described in detail by Company et al. (2017), so
137 we only provide a brief description here. The experiment was carried out at the Hawkesbury
138 Forest Experiment site (33°37'S 150°44'E) in Richmond, NSW, Australia. The site is located
139 in the sub-humid temperate region and experiences warm summers and cool winters. The
140 seedlings were planted on 21st January 2013 (mid-summer) and harvested on 21st May 2013
141 (late autumn). Mean daily temperatures ranged from 22.8 to 46.4 °C (monthly mean of 32.1
142 °C) in January 2013, which was the warmest month of the year, and cooled down in May
143 2013 with an average of 21 °C (BoM, 2017).

144 Twenty-week old *Eucalyptus tereticornis* seedlings in tube stock were chosen from a single
145 local Cumberland plain cohort. Ten seedlings were harvested at the start of the experiment to
146 measure initial leaf area and dry mass of foliage, woody components and roots. Forty-nine
147 seedlings were used in the main experiment, allocated to seven treatments. The plants were
148 grown in containers of differing volume set into the ground (5, 10, 15, 20, 25 or 35 L), or

149 were planted directly into soil (free seedlings, used as the control). All plants were grown in
150 the open under field conditions, but were watered regularly to avoid moisture stress.

151 **2.2 Experimental data acquisition**

152 Full details of all measurements are given in Campany et al. (2017). The mass of each pool
153 (foliage, wood, root, storage) was estimated over time as follows. The initial dry mass of
154 leaves, woods and roots was measured for 10 seedlings at the start of the experiment using
155 the harvesting procedure described in Campany et al. (2017). The dry mass of all
156 experimental plants was measured at the end of the experiment following the same procedure.
157 Seedling growth was tracked during the four months of the experiment, by measuring stem
158 height (h), diameter at 15 cm height (d) and number of leaves on a weekly basis. These
159 measurements were used to estimate the time course of wood and foliage biomass: for root
160 total C we used only initial and final harvest measurements. Initial root C was estimated by
161 averaging all 10 harvested seedlings.

162 We estimated weekly total C in wood ($C_{s,w}$) from the measurements of stem height and
163 diameter, by using an allometric model fitted to initial and final harvest data.

$$\log(C_{t,w}) = b_1 + b_2 \log(d) + b_3 \log(h) \quad (1)$$

164 For each seedling, the total leaf area (LA) and foliage total C ($C_{t,f}$) over time (t) were
165 estimated based on harvested data (T = time of harvest) and weekly leaf counts (LC) over
166 time.

167

$$LA(t) = \frac{LA(T)}{LC(T)} LC(t) \quad (2)$$

$$C_{t,f}(t) = \frac{M_f(T)}{LC(T)} LC(t) \quad (3)$$

168 Fully expanded new leaves were sampled for total non-structural carbohydrate (NSC)
169 concentration on a fortnightly basis. These concentrations were multiplied by leaf biomass to
170 estimate the foliage TNC pool ($C_{n,f}$) at each time point. The partitioning of the non-structural
171 C amongst foliage, wood and root tissues, according to empirically-determined fractions, was
172 then used to estimate the wood and root components of the total TNC pool. Structural C mass
173 for each component was estimated by subtracting non-structural C mass from total C mass.

174 Only foliage non-structural C ($C_{n,f}$) was measured, so to estimate the partitioning of the non-
175 structural C among different organs, we used data from a different experiment on similar-
176 sized seedlings of a related species (*Eucalyptus globulus*), which were grown in 5L pots until
177 four months of age (Duan et al., 2013). We used data from the ambient well-watered control
178 treatments. In that experiment, foliage, wood and root NSC were measured repeatedly over
179 two months. There was no statistically significant change over time in the NSC distribution,
180 so we used the mean distribution for mass-specific C_n over time, which was calculated to be a
181 ratio of 75:16:9 among foliage, wood and root pools.

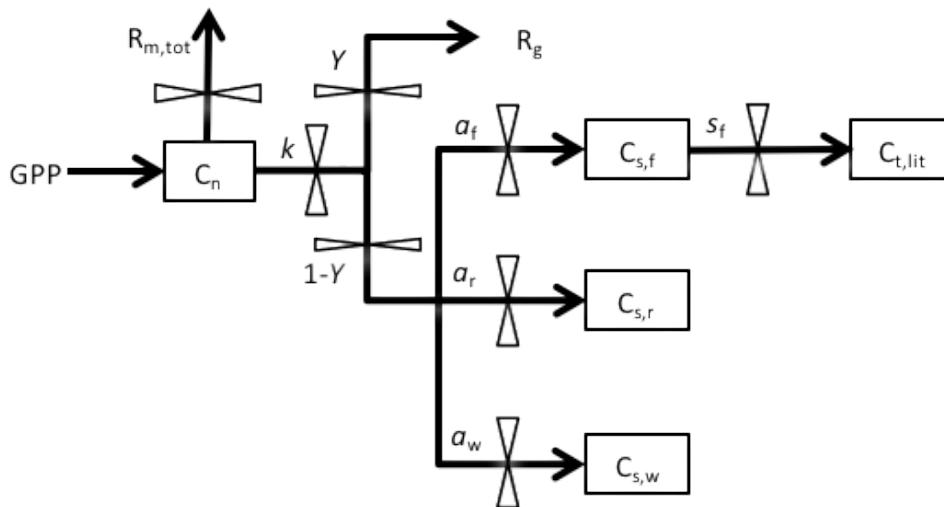
182 We estimated daily GPP from leaf-level gas exchange measurements and a simple canopy
183 scaling scheme as described in Company et al. (2017), and summarized below. Measurements
184 of photosynthesis were made fortnightly throughout the experiment on one fully expanded
185 leaf per plant (Company et al., 2017). Photosynthetic CO_2 response (ACi) curves and leaf
186 dark respiration rates (R) were measured on two occasions, 13-14th March 2013 (when new
187 leaves were first produced) and 14-15th May 2013 (prior to the final harvest). The ACi curves
188 were used to estimate photosynthetic parameters (the maximum rate of Rubisco
189 carboxylation, V_{cmax} and the maximum rate of electron transport for RuBP regeneration under
190 saturating light, J_{max}) using the biochemical model of Farquhar et al. (1980) and fit with the
191 ‘plantecophys’ package (Duursma, 2015) in R. The parameter g_1 , reflecting the sensitivity of
192 stomatal conductance (g_s) to the photosynthetic rate, was estimated by fitting the optimal
193 stomatal conductance model of Medlyn et al. (2011) to measured stomatal conductance data.

194 Treatment effects on photosynthesis were detected immediately on newly produced (fully
195 expanded) leaves and Company et al. (2017) did not observe variation over time in
196 photosynthetic rates. Hence, the photosynthesis parameters were assumed not to change over
197 time but were specific for each treatment. Therefore, daily net C assimilation per unit leaf
198 area (C_{day}) was estimated by using a coupled photosynthesis–stomatal conductance model
199 (Farquhar et al., 1980; Medlyn et al., 2011) using mean photosynthetic parameters (J_{max} ,
200 V_{cmax} , g_1 and R_d) for each treatment and meteorological data from the onsite weather station.
201 The daily GPP was estimated by multiplying C_{day} , total leaf area (LA) and a self-shading
202 factor. The self-shading factor, which is a linear function of LA, is calculated by via
203 simulation with a detailed radiative transfer model, the ‘YplantQMC’ R package of Duursma
204 (2014) for individual treatment. The leaf maintenance respiration rate (R_m , $g\ C\ g^{-1}\ C\ plant\ d^{-1}$)
205 was calculated for each seedling by scaling the measured rate (R) to air temperature using a

206 Q_{10} value of 1.86 (Campany et al., 2017). The daily total maintenance respiration, $R_{m,tot}$ is
 207 calculated as a temperature-dependent respiration rate, R_m , multiplied by plant biomass. We
 208 assumed the same tissue-specific dark respiration rates for leaf, woody and root tissues for
 209 these seedlings, as was observed for seedlings of this species by Drake et al. (2017).

210 2.3 Carbon Balance Model (CBM)

211 We used a DA-modelling framework, similar to that used by Richardson et al. (2013). This
 212 approach uses a simple carbon balance model shown in Figure 1. The model is driven by
 213 daily input of gross primary production (GPP), which directly enters into a non-structural C
 214 pool (C_n). The daily total maintenance respiration, $R_{m,tot}$, is subtracted from C_n pool. The pool
 215 is then utilized for growth at a rate k (i.e. kC_n). Of the utilization flux, a fraction Y is used in
 216 growth respiration (R_g), and the remaining fraction ($1-Y$) is allocated to structural C pools
 217 (C_s): among foliage, wood and root ($C_{s,f}$, $C_{s,w}$, $C_{s,r}$). The foliage pool is assumed to turn over
 218 with rate s_f . We assume there is neither wood or root turnover as the seedlings in the
 219 experiment were young.



220

221 **Figure 1:** Structure of the Carbon Balance Model. Pools, shown as boxes: C_n , non-structural
 222 storage C; $C_{s,f}$, structural C in foliage; $C_{s,r}$, structural C in roots; $C_{s,w}$, structural C in wood.
 223 Fluxes, denoted by arrows, include: GPP, gross primary production; $R_{m,tot}$, total maintenance
 224 respiration; R_g , growth respiration; $C_{t,lit}$, structural C in leaf litterfall. Fluxes are governed by
 225 six key parameters: k , storage utilization coefficient; Y , growth respiration fraction; a_f ,
 226 allocation to foliage; a_w , allocation to wood; a_r , allocation to roots; s_f , leaf turnover rate. a_r is
 227 defined as $1 - a_f - a_w$.

228 The dynamics of the four carbon pools are described by four difference equations:

$$\Delta C_n = GPP - R_m(C_{t,f} + C_{t,w} + C_{t,r}) - k C_n \quad (4)$$

$$\Delta C_{s,f} = k C_n (1 - Y) a_f - s_f C_{s,f} \quad (5)$$

$$\Delta C_{s,w} = k C_n (1 - Y) a_w \quad (6)$$

$$\Delta C_{s,r} = k C_n (1 - Y) a_r \quad (7)$$

229 Where GPP is the gross primary production ($\text{g C plant}^{-1} \text{d}^{-1}$); R_m is the maintenance
 230 respiration rate ($\text{g C g}^{-1} \text{C d}^{-1}$); $C_{t,f}$, $C_{t,w}$, and $C_{t,r}$ are the total C in foliage, wood and root
 231 respectively (g C plant^{-1}); k is the storage utilization coefficient ($\text{g C g}^{-1} \text{C d}^{-1}$); Y is the
 232 growth respiration fraction; a_f , a_w , a_r are the allocation to foliage, wood and root respectively;
 233 and s_f is the leaf turnover rate ($\text{g C g}^{-1} \text{C d}^{-1}$). a_r is defined as $1 - a_f - a_w$.

234 The non-structural (storage) C pool (C_n) is assumed to be divided amongst foliage, wood and
 235 root tissues ($C_{n,f}$, $C_{n,w}$, $C_{n,r}$) according to an empirically-determined ratio of 75:16:9. Total
 236 carbon in each tissue (C_t) is then calculated as the sum of non-structural carbon (C_n) and
 237 structural carbon (C_s) for that tissue.

$$C_{t,f} = 0.75 \times C_n + C_{s,f} \quad (8)$$

$$C_{t,w} = 0.16 \times C_n + C_{s,w} \quad (9)$$

$$C_{t,r} = 0.09 \times C_n + C_{s,r} \quad (10)$$

238 2.4 Application of Data Assimilation (DA) algorithm

239 DA was used to estimate the six parameters (k , Y , a_f , a_w , a_r , s_f) of the CBM for this
 240 experiment. All parameters were allowed to vary quadratically with time, i.e. each parameter
 241 was represented as:

$$p = p_1 + p_2 t + p_3 t^2 \quad (4)$$

242 Quadratic variation over time was found to yield significantly better model fits than either
 243 constant parameter values or linear variation over time (see supplementary section S1). We
 244 executed three distinct sets of model simulations (Table 1), with the goals of (1) testing the
 245 need for a storage pool; (2) determining the effect of sink limitation on model parameters;
 246 and (3) attributing the overall effect of sink limitation on growth to the change in individual
 247 parameters.

248 For each set of model simulations, GPP and R_m were used as inputs to the DA framework,
249 and the measurements of total C mass of each of the plant components and foliage NSC
250 concentrations were used to constrain the parameter values. The set of constraints included 18
251 measurements of $C_{t,f}$ and $C_{t,w}$, two measurements of $C_{t,r}$ (start and end of the experiment), and
252 six measurements of foliage NSC. There were 5 quadratically-varying parameters to
253 determine for each **treatment**, summing to a total of 15 (3x5) coefficients to determine,
254 compared with total 44 data measurements available, for each treatment.

255 We used the Metropolis algorithm (Metropolis et al., 1953) as implemented by Zobitz et al.
256 (2011), with broad prior Probability Density Functions (PDFs) for the parameters (Table 2).
257 Values of k , a_f , a_r and s_f were allowed to vary within the maximum possible range, while
258 parameter Y was constrained according to the literature on growth respiration (Villar and
259 Merino, 2001). Parameter a_r was calculated from a_f and a_w with a check on a_r to ensure that
260 it had reasonable values ($0 < a_r < 1$). Standard Error (SE) was used as an estimate of
261 uncertainty on the assimilated data (Rowland et al., 2014; Richardson et al., 2010), and was
262 calculated based on six replicate measurements. When combining errors, the errors were
263 assumed to be uncorrelated (Hughes and Hase, 2010).

264 Model parameters were assumed to be real, positive and to have a lognormal probability
265 distribution (Rowland et al., 2014). Therefore, all processes of parameter selection, and
266 acceptance and rejection of parameters in relation to prior ranges were performed in
267 lognormal space (Knorr and Kattge, 2005). We performed the first iteration starting from the
268 prior set of parameters. To generate subsequent values for each parameter, a new point was
269 generated by varying all vector elements by some step, chosen with a Gaussian distributed
270 random number generator having a mean of 0 and a SD of 0.005 in log-normal space. We
271 adjusted the step length for each parameter to values which lead to an average acceptance rate
272 of the new points around 35–40%. We confirmed the chain convergence, having 3000
273 iterations to adequately explore the posterior parameter space, by visual inspection of the
274 trace plots of different parameters as suggested by Van Oijen (2008). The trace plots show
275 how the chain moves through parameter space for each individual parameter. The parameter
276 vectors sampled during the first phase of the chain were not representative and therefore the
277 first 10% of the chain was discarded from the posterior sample.

278 **Table 1:** Summary of the three model simulation sets

Simulation Set	Goal	Features	Addressing hypothesis
A	Test importance of storage pool	<ul style="list-style-type: none"> • DA applied to estimate parameters for model without storage pool and model with storage pool • Three treatment groups • Not constrained with NSC data • No leaf area feedback 	H1
B	Identify effect of sink limitation on model parameters	<ul style="list-style-type: none"> • DA applied to estimate parameters for model with storage pool • Data divided into one, two, three or seven treatment groups • Constrained with NSC data • No leaf area feedback 	H2-H5
C	Attribute overall effect on growth to changes in individual parameters	<ul style="list-style-type: none"> • Forward model runs to quantify impact of individual processes on overall plant growth • 5L and free seedlings treatments considered • Parameters changed individually and sequentially • Leaf area feedback on photosynthesis and R_m 	

279 **Table 2:** Prior parameter PDFs (with uniform distribution) and the starting point of the
280 iteration for all parameters

Parameter	Minimum	Maximum	Starting value
k	0	1	0.5
Y	0.2	0.4	0.3
a_f	0	1	0.5
a_w	0	1	0.5
s_f	0	0.01	0.005
$a_r = 1 - (a_f + a_w)$, where $0 < a_r < 1$			

281 **2.4.1 Importance of storage pool**

282 We tested the hypothesis (H1) on the importance of including a non-structural C storage pool
283 in CBM by contrasting fits of the full model with fits of a simplified model without the non-
284 structural C pool (Simulation Set A, Table 1). The simplified model omits the non-structural
285 C pool (C_s) from the full model (Figure 1) and assumes that all available C is utilized for
286 growth each day. We applied the DA framework to both model options and calculated the
287 Bayesian Information Criterion, BIC (Schwarz, 1978) to determine the better model structure.
288 BIC measures how well the model predicts the data based on a likelihood function and
289 compare model performance taking into account the number of fitted parameters, with the
290 lowest BIC number indicating the best model setting. For this comparison, both models were
291 fit to the biomass data only, not leaf NSC data, in order to ensure that both models were fit to
292 the same number of data points.

293 **2.4.2 Effects of sink limitation on model parameters**

294 The effects of sink limitation on C balance were investigated by applying the DA framework
295 to data from all treatments combined, and then subsets of treatments (Simulation Set B, Table
296 1). Considering all treatments pooled together gives same parameters for all the treatments
297 and effectively assumes no effect of sink limitation. On the other hand, taking more subsets
298 of treatments produces more parameter sets (one for each subset) and allows for parameters
299 to vary according to the degree of sink limitation. We first fitted the model to all data,
300 ignoring treatment differences; then considered 2 treatment groups (free seedling / 5-35 L
301 containerized seedlings), 3 groups (free / 5–15 L / 20–35 L) and 4 groups (free / 5-10 L / 15-
302 20 L / 25-35 L). We also fitted the model to each of the 7 treatments individually, where the
303 parameter set for each treatment is unique. The BIC values were compared across treatment
304 groupings.

305 2.4.3 Attribution analysis

306 We performed a sensitivity analysis to quantify the impact of the response of each individual
307 process to sink limitation on overall plant growth (Simulation Set C, Table 1). This analysis
308 consisted of forward runs of the model, including a leaf area feedback to GPP. That is, rather
309 than taking GPP based on measured LA (Eq. 9) as input, in this version of the model we
310 calculated daily GPP using the modelled LA, the photosynthesis rate and corresponding self-
311 shading factor. Adding the LA feedback to the model was necessary to quantify how the
312 treatment effect on individual model parameters affects final seedling biomass through its
313 effect on foliage mass, and consequently GPP, over time.

314 LA in each time step is estimated from NSC-free specific leaf area (SLA_{nonsc}) and the
315 predicted foliage structural carbon ($C_{s,f}$) in that time step. SLA_{nonsc} is calculated at harvest
316 discarding the foliage NSC portion and is assumed to be constant for a given treatment
317 throughout the experiment.

$$LA = SLA_{nonsc} \times C_{s,f} \quad (12)$$

318 Once the LA feedback was implemented in the CBM, we ran the model with the inputs and
319 modelled parameters from the smallest pot seedling (5 L), then changed the parameters to
320 those for the free seedling sequentially in order to quantify the effect of each parameter on the
321 final seedling biomass. The parameters we considered for this attribution analysis were: daily
322 photosynthetic rate per unit leaf area (C_{day}), maintenance respiration rate (R_m), C allocation
323 fractions to biomass (a_f , a_w , a_r), growth respiration rate (Y), foliage turnover rate (s_f) and
324 utilization coefficient (k). We additionally carried out a sensitivity analysis in which we
325 varied each parameter from its baseline value separately.

326

327 3 Results

328 3.1 Importance of storage pool

329 First, we tested the null hypothesis (H1) that there is no need for a non-structural
330 carbohydrate storage pool in the carbon balance model. We compared BIC values for model
331 structures with and without a storage pool. Table 3 (Simulation Set A) shows the results for
332 model fits with the optimal grouping strategy (three treatment groups). BIC values were
333 consistently lower for the model including the storage pool; the improvement in model fit is
334 most noticeable for the containerized seedlings. This analysis demonstrates that the model
335 does need to include a storage pool to correctly represent the experimental data. In all
336 remaining analyses, the full CBM (with non-structural C pool) is applied to data from all four
337 plant C pools (NSC, foliage, wood and root biomass).

338 **Table 3:** BIC values from model fits. The lowest BIC values indicate the best performing
339 parameter settings for any particular simulation. Note that, for Sim A, leaf NSC data were not
340 used to constrain either model, to ensure that both models were fit to the same dataset,
341 resulting in lower BICs compared to Sim B. Treatment groups are: ‘Small’ - 5 L, 10 L and 15
342 L containers; ‘Large’ - 20 L, 25 L and 25 L containers; ‘Free’ – freely rooted seedlings; ‘All’
343 - all data; ‘Containerized’ - all plants in containers.

Simulation Set	Model Setting	Treatment groups	BIC
Sim A	Model without storage pool	Small	459
		Large	550
		Free	182
	Model with storage pool	Small	215
		Large	338
		Free	167
Sim B	7 treatments combined	All	2768
	2 groups	Containerized	1813
		Free	170
		Total	1983
	3 groups	Small	683
		Large	457
		free	170
		Total	1310
7 treatments individually	5 L	85	

		10 L	98
		15 L	60
		20 L	63
		25 L	106
		35 L	152
		Free	170
		Total	734

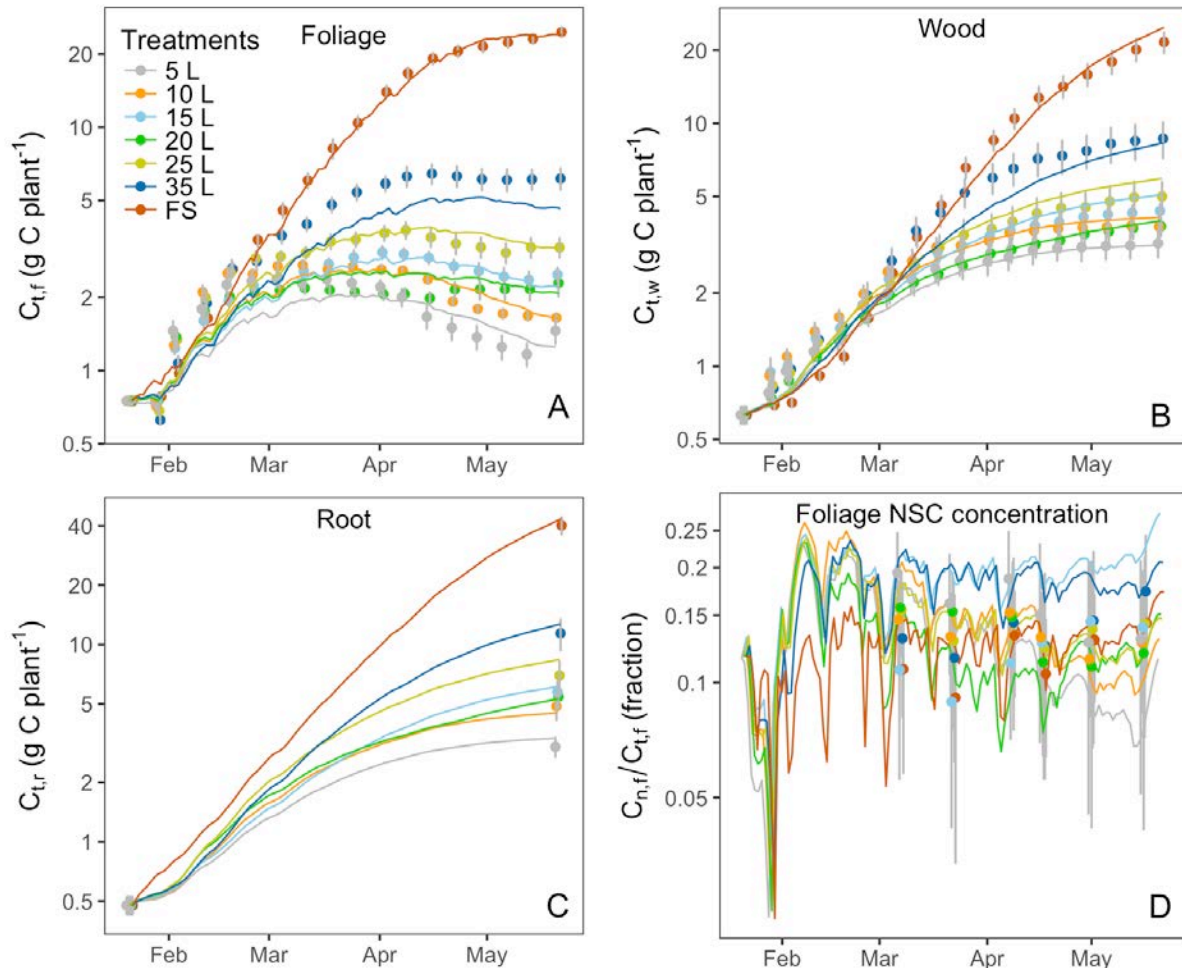
344 **3.2 Sink limitation effect on C balance processes**

345 We addressed our second null hypothesis (H2), that there is no effect of sink limitation on
346 carbon balance processes, by comparing BIC values obtained for model fits when all
347 treatments were combined vs separating the treatments into sub-groups. If there was no effect
348 of sink limitation, the BIC value when all treatments are fit together would be similar to that
349 obtained when treatments are separated into groups. The BIC values shown in Table 3
350 (Simulation Set B) decrease strongly as number of treatment groups increases, indicating a
351 clear effect of sink limitation on carbon balance processes. Although the BIC values continue
352 to decrease as more treatment groups are considered, we also found that interpreting
353 parameter changes became more difficult as the number of groups increased. Hence, further
354 analyses in this paper used unique parameter sets for three treatment groups: small containers,
355 large containers, and free seedlings.

356 **3.3 Analysis of carbon stock dynamics**

357 Figure 2 shows the correspondence between modeled C pools and data. The model
358 reproduced the key features of biomass growth over time in response to treatment. Biomass
359 growth (Figure 2A, B and C) and the foliage storage pool (Figure 2D) were very clearly
360 impacted by sink limitation: biomass growth was strongly reduced for containerised
361 seedlings, which was very well mimicked by the model. Foliage growth in the free seedlings
362 slowed towards the end of the experiment. Wood and root growth continued throughout the
363 experiment in freely-rooted seedlings but slowed down during the second half of the
364 experiment in containerized seedlings. NSC concentrations ($C_{n,f} / C_{t,f}$) in seedlings in small
365 containers were higher compared those in free seedlings at the beginning of the season but all
366 treatments had similar concentrations after four months (Figure 2D). In March, at the time of
367 the first leaf NSC measurements, the foliage storage pool (Supplementary Figure S1) was
368 similar in size across all treatments, but it increased over time in the free seedlings as these
369 plants continued to grow, and decreased over time in the plants in small containers.

370 Modelled C stocks for all 7 treatments closely tracked their corresponding observations
 371 (Figure 2) as most of the predicted biomass values were within one standard error of the
 372 measurements. The exception is the 35 L container treatment, which is underestimated
 373 slightly because the grouping of 20, 25 and 35 L treatments into one group makes it difficult
 374 for the model to fit all treatments in this group.



375

376 **Figure 2:** C stocks (lines) with the inferred parameter set and corresponding observations
 377 (symbols): (A) total C mass in foliage $C_{t,f}$, (B) total C mass in wood $C_{t,w}$, (C) total C mass in
 378 root $C_{t,r}$ and (D) foliage NSC concentration ($C_{n,f}/C_{t,f}$). Note that the carbon pools and foliage
 379 NSC concentration (y-axes) are plotted on log scale to visualize the changes at the beginning
 380 of the experiment. Error bars (1 SE, $n = 6$) are shown for each observation.

381

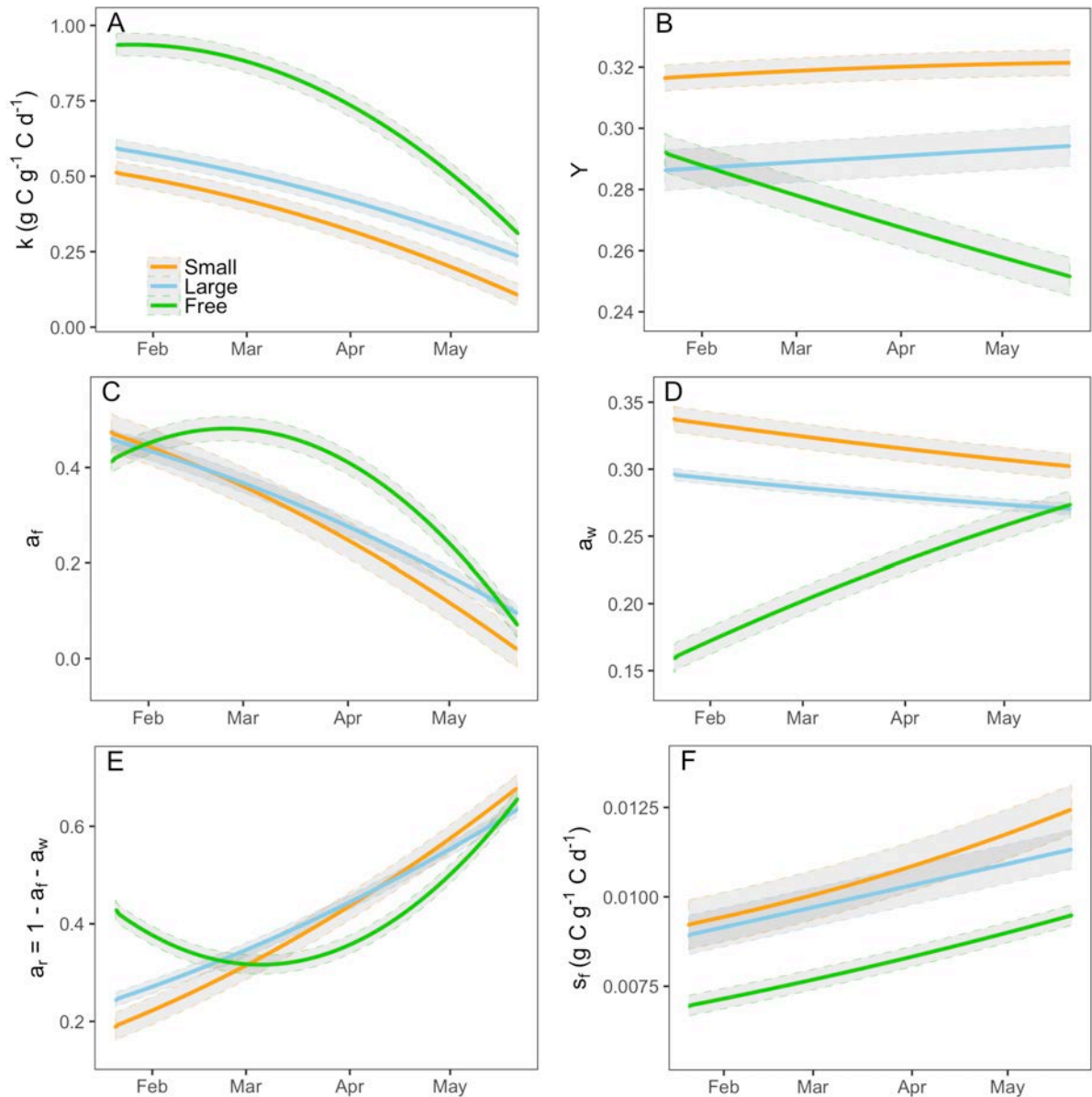
382 3.4 Parameter estimates

383 Data assimilation indicated significant treatment effects on all five fitted parameters (Figure
384 3). There was a large effect of sink limitation on the utilization coefficient (k). In agreement
385 with our hypothesis H3, the free seedling had the highest k , and the seedlings in small
386 containers (most sink limited) had the lowest k (Figure 3A). As the experiment progressed,
387 the utilization rate of free seedlings began to decrease (Figure 3A). In contrast to the free
388 seedlings, the potted seedlings had relatively low utilization rates initially (k close to 0.5) and
389 the utilization rates slowed down abruptly with time, most significantly in the smallest
390 container treatments (Figure 3A).

391 In agreement with hypothesis H4, the estimated growth respiration rate (Y) varied according
392 to the sink strength of the treatment groups, and was highest in the lowest sink strength
393 treatments (Figure 3B). Moreover, Y did not vary significantly over time for the sink limited
394 treatment groups. However, the rate of growth respiration for the free seedling slowed down
395 over time.

396 The data assimilation process also indicated that the growth allocation fractions vary among
397 treatments and over time. Consistent with hypothesis H5, wood allocation fraction was
398 highest in the smallest container treatments, and lowest in the free seedlings (Figure 3D). For
399 the free seedlings, allocation was initially highest to foliage and roots (Figure 3C-E); over
400 time, the plants reduced allocation to foliage and increased it to wood and roots. In the
401 containerized seedlings, allocation was initially highest to wood and foliage; over time,
402 foliage allocation decreased to almost zero and root allocation increased.

403 The estimated leaf turnover rate, s_f was also notably higher for sink-limited treatments
404 compared to free seedlings (Figure 3F). The large value of modelled leaf litterfall for sink-
405 limited treatments is consistent with observations during the experiment that containerized
406 seedlings had relatively large leaf litterfall, beyond normal senescence. Estimated s_f increased
407 over time for all treatment groups (most notably in free seedlings), due to a combination of
408 ontogeny, seasonal change, and growth restriction in the sink-limited seedlings.



409

410 **Figure 3:** Modelled final parameters for three groups of treatments during the experiment
 411 period (21st Jan to 21st May 2013): (A) storage utilization coefficient, k ; (B) growth
 412 respiration fraction, Y ; (C) allocation to foliage, a_f ; (D) allocation to wood, a_w ; (E) allocation
 413 to roots, a_r and (F) leaf turnover rate, s_f . a_r is defined as $1 - a_f - a_w$. The grey shaded area
 414 shows the 95% confidence intervals of modelled parameters.

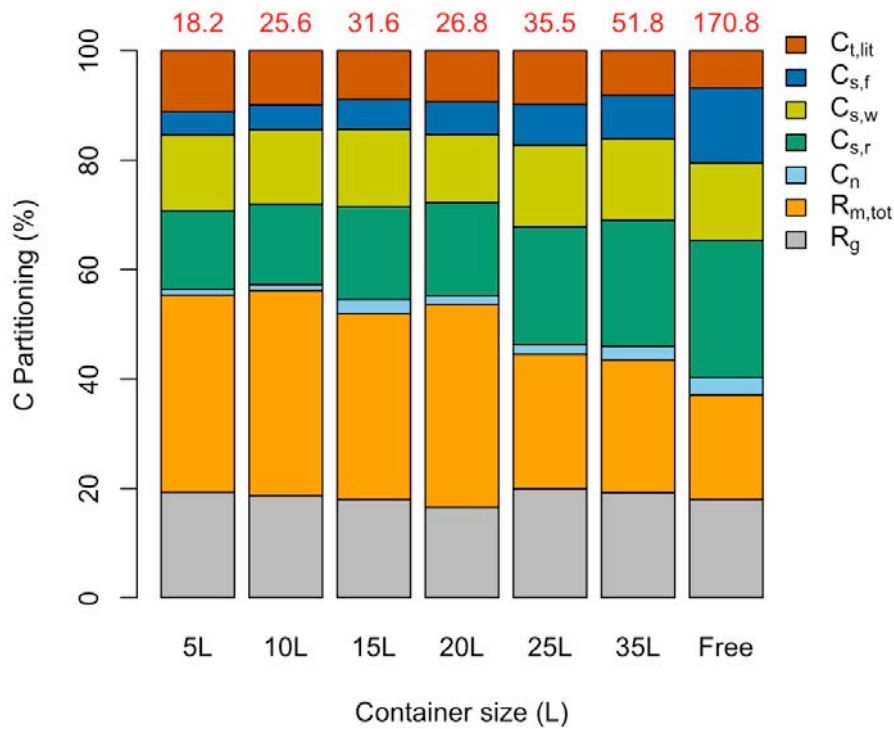
415

416 3.5 Carbon budget

417 The model was used to partition total GPP (g C plant^{-1}) from the entire experiment period
 418 into different C pools (growth respiration, maintenance respiration, non-structural carbon,
 419 structural foliage, wood, and root carbon, and litterfall) for all 7 treatments (Figure 4). Total

420 GPP was considerably lower for the containerized seedlings, owing to lower photosynthetic
421 rates per unit leaf area, C_{day} (Figure 5A), and lower total leaf area (LA) per plant. Though
422 starting with the same total LA of 0.016 m^2 , the 5 L containerized and free seedlings had total
423 LA of 0.031 and 0.516 m^2 respectively after four months of treatment. Simultaneously, the
424 partitioning of GPP changed considerably across different treatments.

425 Small container seedlings (5, 10, 15 L) had a higher fraction of GPP lost in leaf litterfall
426 compared to other seedlings (Figure 4), consistent with observations during the experiment.
427 The proportion of GPP in final foliage mass was extremely low in sink limited treatments
428 (also shown in Figure 2A). Allocation of GPP to final foliage and root biomass were highest
429 in the free seedlings, although interestingly allocation to final wood biomass was similar
430 across treatments. The final allocation to storage was also higher in free seedlings. The sink
431 limited seedlings had a higher proportional C lost through maintenance respiration. Tissue
432 specific respiration rates were similar in free and containerized seedlings, so the $\sim 35\%$
433 reduction in photosynthetic rate for the smallest containerized seedling, led to a higher overall
434 $R_{\text{m.tot}}/\text{GPP}$ fraction. In summary, the estimated total respiration ($R_{\text{m.tot}} + R_{\text{g}}$) to GPP ratio was
435 considerably lower for the free seedlings compared to the sink limited treatments. The carbon
436 use efficiency (CUE) remained relatively constant and high over time for free seedlings
437 (~ 0.65), whereas CUE in the smallest container treatments showed a sharp reduction over
438 time down to ~ 0.25 (Supplementary Figure S2).



439

440 **Figure 4:** Simulated proportional C partitioning for the whole experimental period. The total
 441 accumulated GPP (g C plant⁻¹) for individual treatments is shown (in red) at the top of each
 442 column. Free stands for free seedling. Different C partitions are in the colour legend: total
 443 litterfall, $C_{t,lit}$; foliage structural C, $C_{s,f}$; wood structural C, $C_{s,w}$; root structural C, $C_{s,r}$; non-
 444 structural C pool, C_n ; total maintenance respiration, $R_{m,tot}$ and growth respiration, R_g .

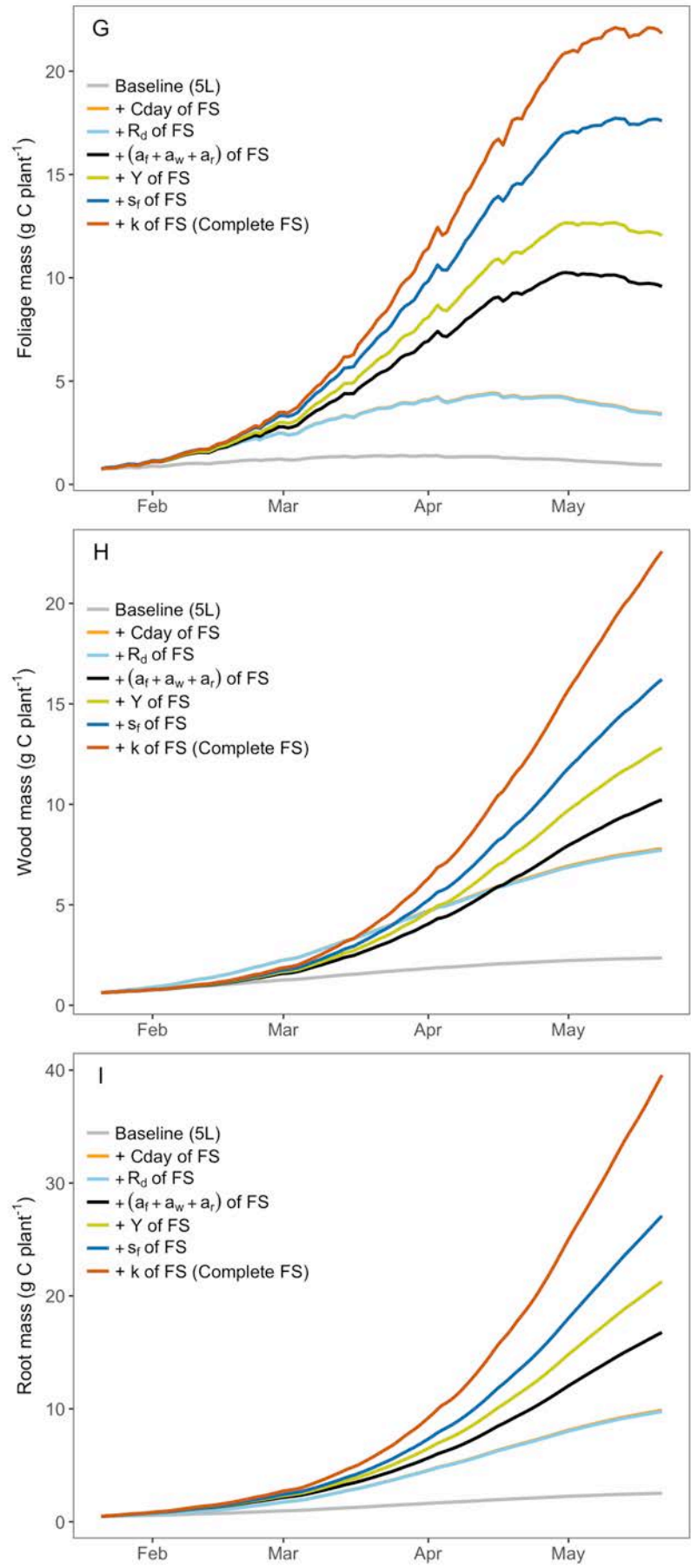
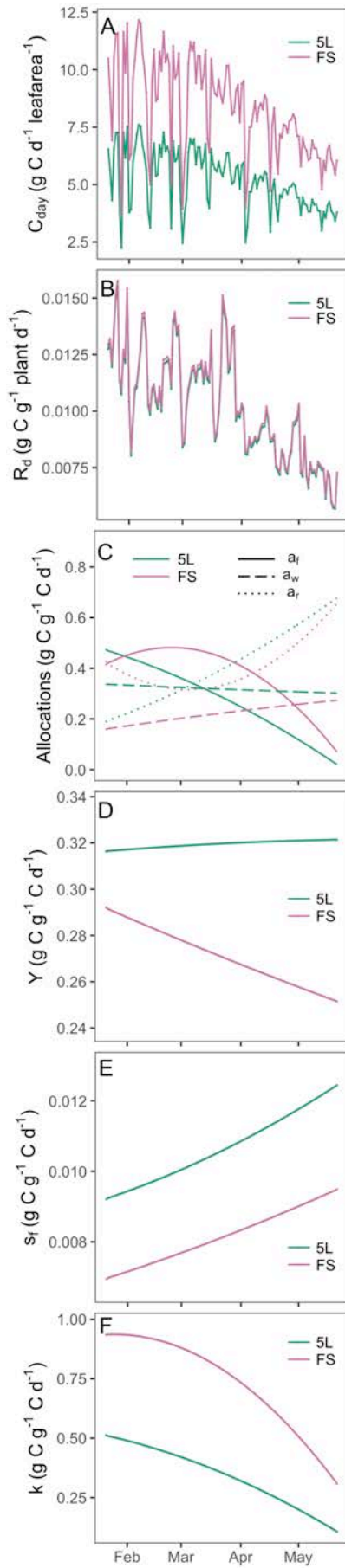
445

446 3.6 Attribution analysis

447 Sink limitation affected biomass growth via a range of processes, namely reduction in
 448 photosynthesis, and variation in the utilization rate, growth respiration, leaf litterfall, and C
 449 allocations to foliage, wood and root across various treatment groups. We quantified the
 450 contribution of each of these process responses separately by running the CBM with
 451 parameter inputs changing both sequentially and individually (one at a time). Table 4 presents
 452 the effect of the parameters changing individually from the value of the smallest container
 453 treatment (5 L) to that of free seedling (FS) and other way around, resetting the previous
 454 parameter to the baseline value. The final biomass values in Table 4 indicate the contribution
 455 of each individual parameter separately and sequentially. Photosynthetic capacity had the
 456 largest individual effect on total plant growth (+15.28 and -71.9 g C) compared to the rest of

457 the parameters. However, allocation pattern and the utilization rate also had a sizeable effect
458 on final biomass (Table 4).

459 Figure 5 shows how biomass (M_f , M_w and M_r) is predicted to change when each parameter is
460 changed sequentially from the parameter set derived from DA on the 5L observations (gray
461 line, Figure 5) to that of the parameters obtained when using the free seedlings as constraint
462 of the model (red line, Figure 5). Daily net C assimilation per unit leaf area (C_{day}), which was
463 30% higher for free seedling compared to 5 L container treatment (Figure 5A), had a large
464 impact on plant growth (final total biomass was increased by 11 g, Table 4 and Figure 5G-I,
465 gray to orange). Maintenance respiration rate (R_m) did not vary significantly across
466 treatments (Figure 5B), in line with the data presented in Company et al. (2017), and
467 consequently its impact was insignificant (the final total biomass is reduced by only 0.24 g,
468 Table 4 and Figure 5G-I, orange to light blue). The modelled biomass allocation fractions (a_f ,
469 a_w and a_r) in Figure 5C had important, but mixed, effects on C stocks. The final foliage mass
470 was increased from 3.4 g to 9.6 g due to the increase in C allocation to foliage (Figure 5G,
471 light blue to green), which has a positive feedback on GPP. Concomitant changes in C
472 allocation to wood and root resulted in smaller changes to these biomasses as shown in
473 Figure 5H-I (2.5 g and 7.0 g rise respectively). Overall, the change in allocation pattern
474 resulted in an increase in final total biomass by 15.74 g (Table 4). Growth respiration rate (Y)
475 was ~20% lower in free seedlings (Figure 5D), which had a considerable impact on C
476 budgets (the final total biomasses were increased by 9.56 g, Table 4 and green to yellow,
477 Figure 5G-I). Leaf turnover, s_f was low in the free seedlings compared to the 5 L container
478 treatment (Figure 5E) which had a large positive effect on final C pools (Figure 5G-I, yellow
479 to blue). The foliage mass was increased by 5.6 g; the wood and root masses were also
480 further increased (3.4 g and 5.8 g respectively) due to the increase in GPP when foliage is
481 retained for longer. Finally, the utilization coefficient, k was higher in free seedlings (Figure
482 5F) causing a 20-30% positive feedback on C budgets (total biomass increased by 23.08 g,
483 Table 4 and Figure 5G-I, blue to red).



485 **Figure 5:** Attribution analysis. Left column (A-F): changes in **inferred parameters**; Right
 486 column (G-I): associated impacts on C budgets **due to sequential parameter changes from 5 L**
 487 **container treatment to that of free seedling** (right column, G-I). Different colours in the figure
 488 indicate the parameter shifts (left column, A-F) and their associated impacts on C budgets
 489 (right column, G-I). Legend: 5L, highly sink-limited treatment with container size of 5 L; FS,
 490 Free Seedling without any sink limitation. Note that the orange line is overlain by the light
 491 blue line: the small change in maintenance respiration results in a very minor effect on
 492 biomass growth.

493 **Table 4:** Estimates of final biomass due to parameter change (individual and sequential),
 494 showing the contribution of each parameter separately and successively to biomass changes.
 495 All values in g C plant⁻¹. +/- indicates biomass increase or decrease due to particular
 496 parameter change. The final column corresponds to the changes shown in Figure 5.

Parameter change	Individually		Sequentially
	5 L » FS	FS » 5 L	5 L » FS
Baseline C _t	5.81	83.99	5.81
C _{day}	+15.28	-71.9	+15.28
R _d	-0.08	+1.1	-0.24
(a _f + a _w + a _r)	+1.53	-45.5	+15.74
Y	+0.41	-19.22	+9.56
s _f	+1.13	-19.17	+14.77
k	+0.44	-23.08	+23.08
FS total observed C _t			83.99

497

498 **4 Discussion**

499 **4.1 Effects of sink limitation on C balance**

500 Our DA-model analysis of this root volume restriction experiment provided significant new
 501 insights in the response of key C balance processes to sink limitation. We were able to infer
 502 that, in addition to a reduction in photosynthetic rates, sink limitation reduced NSC utilization
 503 rates, increased growth respiration, modified allocation patterns and enhanced senescence.
 504 Our attribution analysis indicated that all of these process responses contributed significantly
 505 to the overall reduction in biomass observed under low rooting volume.

506 We first tested the null hypothesis (H1) that seedling growth rates could be adequately
507 predicted from current-day photosynthate. This hypothesis was rejected, with a storage pool
508 being necessary to simulate growth, particularly for containerized seedlings (Sim A, Table 3).
509 The approach of simulating growth from current-day photosynthate is commonly used in
510 models, particularly for evergreen plants (e.g. (Jain and Yang, 2005; Law et al., 2006;
511 Thornton et al., 2007)), but several authors have proposed the need for a storage pool to
512 balance the C sources and sinks in the short term, as well as simulate the effects of
513 photosynthetic down-regulation in the long-term (Pugh et al., 2016; Richardson et al., 2013;
514 Fatichi et al., 2016). Our results support the need for an NSC pool in CBMs.

515 We then tested the second null hypothesis (H2) that there was no effect of treatment on the
516 parameters of the C balance model. This hypothesis was also rejected: fitting the DA-model
517 framework simultaneously to all treatments with one set of parameters (ignoring sink
518 limitation effect) gave a low goodness of fit (Sim B, Table 1). This result is consistent with
519 the finding of Company et al. (2017) that the observed effects of sink limitation on
520 photosynthesis in this experiment were insufficient to explain the large reduction in biomass.
521 Instantaneous photosynthetic rates were reduced 20-30% by sink limitation. Our DA analysis
522 indicated that several other processes contributed to the reduction in biomass growth,
523 including carbohydrate utilization, growth respiration, allocation patterns, and turnover.

524 Our results suggested a significant effect of sink limitation on the carbohydrate utilization
525 rate, k (Figure 3A). The modelled k values were approximately twice as large in free
526 seedlings compared to the small containers. This result supports the hypothesis (H3) that
527 plants would have the lowest utilization rate under sink-limited conditions. At the start of the
528 measurement period, the free seedlings were utilizing almost all C produced immediately in
529 growth (k close to 1.0, Figure 3A). The utilization coefficient of the free seedlings decreased
530 over time, causing a build-up in C storage (Figure 2D). This decrease in utilization rate could
531 potentially be an ontogenetic effect, with free seedlings initially allocating all carbon to
532 growth during establishment but increasing storage with increasing size. However,
533 ontogenetic effects are confounded with season in this experiment, such that decreasing
534 utilization rates over time could also be a result of decreasing temperatures moving into
535 autumn. There is a real need to quantify how the carbohydrate utilization rate varies with
536 environmental conditions and ontogeny; data assimilation of experiments in which
537 photosynthesis and growth rates have been monitored over time offer one means to do so.

538 Although the carbohydrate utilization rate was highest in the free seedlings, leaf carbohydrate
539 concentrations were not lower in these plants at the end of the experiment. As shown in the
540 final C budget analysis (Figure 4), there was a higher total C allocation to the NSC pool in
541 free seedlings than sink-limited treatments. Final carbohydrate storage was high in free
542 seedlings despite high k because the carbohydrate pool was recharged throughout the
543 experiment (Figure 2D), as the free seedlings had high photosynthetic rates but no higher
544 maintenance respiration requirement. In contrast, NSC was depleted for the smallest pot
545 treatments after mid-March (Figure 2D) when demand exceeded supply due to both limited
546 production of photoassimilates and enhanced leaf litterfall (Figure 3F).

547 The modelled rate for growth respiration, Y was larger for sink limited treatments than the
548 free seedling (Figure 3B). Overall, there was lower C utilization (i.e. CUE) in plant structural
549 growth in sink-limited treatments (~45%) compared to free seedlings (~60%). This finding
550 supports the “wasteful plant” hypothesis H4. Inferred Y remained constant over time for the
551 containerized treatments, implying a fixed portion of C loss due to growth respiration despite
552 seasonal variation. However, a reduction in Y over time was inferred for the free seedling,
553 suggesting a possible ontogenetic effect. However, it is important to note that we have
554 inferred growth respiration from the CBM framework. Therefore, these estimates could
555 possibly also include C losses via other pathways. Direct measurements of growth respiration
556 rates would be useful to confirm the inferred effects of sink limitation and investigate
557 potential underlying mechanisms.

558 We also demonstrated that the allocation fractions among organs change in sink-limited
559 conditions, with sizeable consequences for plant growth rates. Previous analyses of pot-size
560 experiments have generally only been able to estimate changes in final biomass partitioning
561 (e.g. Poorter et al. 2012a). Company et al. (2017) analysed final biomass partitioning in the
562 experiment and did not find any significant difference in biomass partitioning in sink-limited
563 seedlings compared to free seedlings, once ontogenetic drift was taken into account. Our
564 analysis adds to that of Company et al. (2017) by calculating the dynamics of allocation over
565 time and taking estimated foliage loss into account. Our analysis showed that modelled
566 allocation fractions vary significantly over time (Figure 3C, D and E). In the free seedlings,
567 allocation to foliage decreased, and allocation to both wood and roots increased, reflecting
568 the ontogenetic effects mentioned by Company et al. (2017). However, our analysis also
569 highlights significant variations among treatments in the modelled C allocation fractions to

570 foliage, wood and root that are not ontogenetic. At the beginning of the experiment, foliage
571 allocation fractions were similar for all treatment groups, but wood allocation was higher, and
572 root allocation lower, in the containerized seedlings compared to the free seedlings. For the
573 containerized seedlings, changes over time also differed from those in the free seedlings:
574 wood allocation decreased marginally, rather than increasing, foliage allocation declined
575 steeply over time, and root allocation increased steeply. These allocation patterns in seedlings
576 supported our hypothesis H5 that sink limitation due to root restriction would favour
577 allocation to wood over foliage or fine roots. Calculating dynamic allocation patterns over the
578 course of an experiment thus provides additional insights beyond analysis of the final
579 biomass outcome.

580 **4.2 Application of DA to infer C balance processes**

581 We have demonstrated that the DA approach can be an invaluable tool for quantifying C
582 fluxes in experimental systems, enabling us to extract important new information from
583 existing datasets to inform carbon balance models, such as the rate and timing of the transfer
584 of photosynthate to and from storage pools. The DA-modelling approach is able to draw
585 together the experimental data to estimate all the components of C balance, including
586 photosynthesis, respiration, NSC, biomass partitioning and turnover. This approach could
587 readily be applied to other experiments to derive new information allowing better
588 representation of C balance processes in vegetation models.

589 Applying this approach requires a range of measurements to constrain the key C balance
590 processes. Here, we used estimated daily C assimilation and maintenance respiration rate as
591 model inputs and constrained the model with measurements of biomass pools (foliage, wood,
592 root) and foliage NSC concentrations. We used fortnightly foliage and wood biomass
593 measurements; the DA framework would work with fewer data observations, but parameters
594 would be estimated with less accuracy. Informal exploration of the model suggested that
595 measurements of foliage turnover would have been particularly useful to better constrain the
596 model. Any experiment having estimates of GPP, maintenance respiration, and structural
597 biomass could potentially be investigated with this framework. However, additional
598 measurements of storage and turnover would be highly beneficial for the performance of the
599 simulation. Repeated observations over time are also useful, particularly for young plants, to
600 account for variations in parameter values over time. We found significant changes in

601 parameter values during the course of the 4-month experiment, which may be linked to both
602 ontogeny and seasonal variation in temperature.

603 One major caveat on our results is that below-ground carbon cycling processes were not well
604 characterized. For practical reasons, processes such as root growth, respiration, turnover, and
605 exudation are rarely well quantified in empirical studies. Here, we had access to initial and
606 final estimates of root biomass. Root respiration was estimated; root turnover and exudation
607 were assumed to be zero. There is evidence that stress can increase rates of root exudation:
608 for example, Karst et al. (2016) demonstrate increased exudation rates in seedlings exposed
609 to cold soils. They also showed that stressed plants may exude C beyond that predicted by
610 simple concentration gradients in NSC between root and soil. The loss of C independent of
611 NSC in roots suggests that exudation may be actively enhanced once plant growth is limited
612 (Hamilton et al., 2008; Karst et al., 2017). As our CBM does not include this process, it
613 would attribute any C loss through root exudation to another process removing C from the
614 plant, such as growth respiration. The increase in growth respiration that we inferred may
615 thus potentially include root exudation. We have reasonable confidence, from the
616 combination of measurements available, in our inference that the C loss term was increased
617 with sink limitation. However, direct measurements of one or both processes would be
618 required to determine the role of root exudation.

619 In addition, we did not have access to estimates of root or wood NSC. We used data
620 measured in a previous experiment on 4-month old *E. globulus* seedlings (Duan et al. 2013)
621 to estimate these values from foliage NSC. It would have been useful to obtain these values,
622 particularly since wood and root tissue can act as storage organs, and the timing of storage
623 development would be extremely useful to quantify. The concentration of NSC in plant roots
624 measured by Duan et al. (2013) was relatively small compared to that of foliage (mean
625 2.15%). However, fine root NSC values in a nearby experiment on 17-month-old *E.*
626 *parramattensis* saplings were even lower (0.78%) (Morgan E. Furze et al. unpublished data).
627 It is possible that these very fast-growing Eucalypt species only start to accumulate root
628 reserves when they are established. Further research is needed to quantify the trade-off
629 between allocation to growth and storage during establishment.

630 **4.3 Implications for modelling plant growth under sink limited conditions**

631 The goal of our study was to examine how carbon balance models should be modified to
632 represent sink limitation of growth, whilst maintaining mass balance. Our results demonstrate
633 that several process representations need to be modified. Firstly, we demonstrate a clear need
634 to incorporate a carbohydrate storage pool, with a dynamic utilization rate for growth. We
635 demonstrate that the utilization rate is slowed by sink limitation, and may also vary with
636 ontogeny. Targeted experimental work is needed to better quantify this variation in utilization
637 rates. Secondly, in addition to a feedback on photosynthetic rates, other plant processes
638 including growth respiration, turnover and allocation are also affected by sink limitation.
639 Applying a DA-modelling framework to experimental data with rooting volume restriction
640 has allowed us to quantify these effects in this experiment. Applying this approach more
641 broadly would potentially allow us to identify general patterns that could then be formulated
642 for inclusion into models.

643 The inferences on carbohydrate dynamics from seedling studies could be used to infer mature
644 tree responses that can subsequently be integrated at ecosystem level and beyond using the
645 concepts of Hartmann et al. (2018). We are enthusiastic to see the approach applied to other
646 experiments, but there are likely to be gaps in the datasets to constrain the key C balance
647 processes. Fortunately, the DA approach does not require continuous measurements of all of
648 the C stocks and fluxes. In the absence of measurements, the model can be relied upon to
649 project the time evolution of missing stocks and fluxes, although of course, the precision of
650 model estimates and insights that can be gained, increases with data availability. DA can also
651 be applied at ecosystem scale. There are several successful examples of DA being applied to
652 forest growth, albeit without a focus on storage (e.g. Van Oijen (2008); Williams et al.
653 (2005); Bloom et al. (2016); Quaipe et al. (2008); Pinnington et al. (2016)). Overall, this
654 approach provides important insights into the regulation of carbohydrate storage and would
655 significantly advance our ability to predict the impacts of environmental changes on plant
656 growth and vulnerability to stress.

657 **Data availability**

659 The raw data are freely available on Figshare (doi:
660 <https://doi.org/10.6084/m9.figshare.5125087.v3>). The R source code to perform all the data
661 processing and analysis to replicate the figures is freely available as a Git repository
662 (https://github.com/kashifmahmud/DA_Sink_limited_experiment).

663

664 **Author contribution**

665 KM analyzed the data, developed the model code, performed the simulations and wrote the
666 paper. BEM conceived the idea and helped in data analysis. RAD and CC provided the
667 experimental data. BEM, RAD, CC and MGD provided in-depth editing of the manuscript.

668

669 **Competing interests**

670 The authors declare that they have no conflict of interest.

671

672 **Acknowledgements**

673 This research was supported by the Australian Research Council (Discovery, DP
674 DP160103436), the Hawkesbury Institute for the Environment, and Western Sydney
675 University. The authors wish to thank Burhan Amiji for his technical assistance and all
676 individuals from Hawkesbury Institute for the Environment who helped during the
677 experimental harvest. We thank Mathew Williams for advice on implementing the data
678 assimilation framework.

679

680 **References**

681 Arp, W. J.: Effects of source sink relations on photosynthetic acclimation to elevated carbon
682 dioxide, *Plant, Cell and Environment*, 14, 869-876, 1991.

683 Bloom, A. A., Exbrayat, J.-F., van der Velde, I. R., Feng, L., and Williams, M.: The decadal
684 state of the terrestrial carbon cycle: Global retrievals of terrestrial carbon allocation, pools,
685 and residence times, *Proceedings of the National Academy of Sciences*, 113, 1285-1290,
686 10.1073/pnas.1515160113, 2016.

687 BoM: Climate Data Online (Station 067105), Bureau of Meteorology Melbourne.

688 <http://www.bom.gov.au/climate/data/> (Accessed 26-08-2017). 2017.

689 Bossel, H.: treedyn3 forest simulation model, *Ecol. Model.*, 90, 187-227,

690 [https://doi.org/10.1016/0304-3800\(95\)00139-5](https://doi.org/10.1016/0304-3800(95)00139-5), 1996.

691 Bradford, K. J., and Hsiao, T. C.: Stomatal behavior and water relations of waterlogged
692 tomato plants, *Plant Physiol*, 70, 1508-1513, 1982.

693 Buckley, T. N.: The control of stomata by water balance, *New Phytologist*, 168, 275-292,
694 10.1111/j.1469-8137.2005.01543.x, 2005.

695 Campany, C. E., Medlyn, B. E., and Duursma, R. A.: Reduced growth due to belowground
696 sink limitation is not fully explained by reduced photosynthesis, *Tree Physiol*, 37, 1042-1054,
697 10.1093/treephys/tpx038, 2017.

698 Crous, K. Y., and Ellsworth, D. S.: Canopy position affects photosynthetic adjustments to
699 long-term elevated CO₂ concentration (FACE) in aging needles in a mature *Pinus taeda*
700 forest, *Tree Physiol*, 24, 961-970, 2004.

701 De Kauwe, M. G., Medlyn, B. E., Zaehle, S., Walker, A. P., Dietze, M. C., Wang, Y. P., Luo,
702 Y. Q., Jain, A. K., El-Masri, B., Hickler, T., Warlind, D., Weng, E. S., Parton, W. J.,
703 Thornton, P. E., Wang, S. S., Prentice, I. C., Asao, S., Smith, B., McCarthy, H. R., Iversen,
704 C. M., Hanson, P. J., Warren, J. M., Oren, R., and Norby, R. J.: Where does the carbon go? A
705 model-data intercomparison of vegetation carbon allocation and turnover processes at two
706 temperate forest free-air CO₂ enrichment sites, *New Phytologist*, 203, 883-899,
707 10.1111/nph.12847, 2014.

708 de Wit, C. T.: *Simulation of assimilation, respiration, and transpiration of crops*, Wiley, 1978.

709 de Wit, C. T., and van Keulen, H.: Modelling production of field crops and its requirements,
710 *Geoderma*, 40, 253-265, [https://doi.org/10.1016/0016-7061\(87\)90036-X](https://doi.org/10.1016/0016-7061(87)90036-X), 1987.

711 Drake, J. E., Vårhammar, A., Kumarathunge, D., Medlyn, B. E., Pfautsch, S., Reich, P. B.,
712 Tissue, D. T., Ghannoum, O., and Tjoelker, M. G.: A common thermal niche among
713 geographically diverse populations of the widely distributed tree species *Eucalyptus*
714 *tereticornis*: No evidence for adaptation to climate-of-origin, *Glob. Change Biol.*, 23, 5069-
715 5082, doi:10.1111/gcb.13771, 2017.

716 Duan, H., Amthor, J. S., Duursma, R. A., O'Grady, A. P., Choat, B., and Tissue, D. T.:
717 Carbon dynamics of eucalypt seedlings exposed to progressive drought in elevated [CO₂] and
718 elevated temperature, *Tree Physiol.*, 33, 779-792, 10.1093/treephys/tpt061, 2013.

719 Duursma, R. A.: YplantQMC: plant architectural analysis with Yplant and
720 QuasiMC, 2014.

721 Duursma, R. A.: Plantecophys - An R Package for Analysing and Modelling Leaf Gas
722 Exchange Data, *PLOS ONE*, 10, e0143346, 10.1371/journal.pone.0143346, 2015.

723 Farquhar, G. D., Von Caemmerer, S., and Berry, J. A.: A biochemical model of
724 photosynthetic carbon dioxide assimilation in leaves of 3-carbon pathway species, *Planta*,
725 149, 78-90, 1980.

726 Fatichi, S., Leuzinger, S., and Körner, C.: Moving beyond photosynthesis: from carbon
727 source to sink-driven vegetation modeling, *New Phytologist*, 201, 1086-1095,
728 10.1111/nph.12614, 2014.

729 Fatichi, S., Pappas, C., and Ivanov, V. Y.: Modeling plant–water interactions: an
730 ecohydrological overview from the cell to the global scale, *Wiley Interdisciplinary Reviews:*
731 *Water*, 3, 327-368, doi:10.1002/wat2.1125, 2016.

732 Friend, A. D., Lucht, W., Rademacher, T. T., Keribin, R., Betts, R., Cadule, P., Ciais, P.,
733 Clark, D. B., Dankers, R., Falloon, P. D., Ito, A., Kahana, R., Kleidon, A., Lomas, M. R.,
734 Nishina, K., Ostberg, S., Pavlick, R., Peylin, P., Schaphoff, S., Vuichard, N., Warszawski, L.,
735 Wiltshire, A., and Woodward, F. I.: Carbon residence time dominates uncertainty in
736 terrestrial vegetation responses to future climate and atmospheric CO₂, *Proceedings of the*
737 *National Academy of Sciences*, 111, 3280-3285, 10.1073/pnas.1222477110, 2014.

738 Gunderson, C. A., and Wullschleger, S. D.: Photosynthetic acclimation in trees to rising
739 atmospheric CO₂: a broader perspective, *Photosynthesis Research*, 39, 369-388, 1994.

740 Hamilton, E. W., Frank, D. A., Hinchey, P. M., and Murray, T. R.: Defoliation induces root
741 exudation and triggers positive rhizospheric feedbacks in a temperate grassland, *Soil Biology*
742 *and Biochemistry*, 40, 2865-2873, <https://doi.org/10.1016/j.soilbio.2008.08.007>, 2008.

743 Hartmann, H., McDowell, N. G., and Trumbore, S.: Allocation to carbon storage pools in
744 Norway spruce saplings under drought and low CO₂, *Tree Physiol.*, 35, 243-252,
745 10.1093/treephys/tpv019, 2015.

746 Hartmann, H., and Trumbore, S.: Understanding the roles of nonstructural carbohydrates in
747 forest trees – from what we can measure to what we want to know, *New Phytologist*, 211,
748 386-403, doi:10.1111/nph.13955, 2016.

749 Hartmann, H., Adams, H. D., Hammond, W. M., Hoch, G., Landhäusser, S. M., Wiley, E.,
750 and Zaehle, S.: Identifying differences in carbohydrate dynamics of seedlings and mature
751 trees to improve carbon allocation in models for trees and forests, *Environ. Exp. Bot.*,
752 <https://doi.org/10.1016/j.envexpbot.2018.03.011>, 2018.

753 Hughes, I. G., and Hase, T. P. A.: *Measurements and their Uncertainties A Practical Guide to*
754 *Modern Error Analysis*, Oxford University Press, Oxford, UK, 2010.

755 Jain, A. K., and Yang, X.: Modeling the effects of two different land cover change data sets
756 on the carbon stocks of plants and soils in concert with CO₂ and climate change, *Global*
757 *Biogeochemical Cycles*, 19, n/a-n/a, 10.1029/2004GB002349, 2005.

758 Karst, J., Gaster, J., Wiley, E., and Landhäusser, S. M.: Stress differentially causes roots of
759 tree seedlings to exude carbon, *Tree Physiol.*, 37, 154-164, 10.1093/treephys/tpw090, 2017.

760 Klein, T., and Hoch, G.: Tree carbon allocation dynamics determined using a carbon mass
761 balance approach, *New Phytologist*, 205, 147-159, doi:10.1111/nph.12993, 2015.

762 Knorr, W., and Kattge, J.: Inversion of terrestrial ecosystem model parameter values against
763 eddy covariance measurements by Monte Carlo sampling, *Glob. Change Biol.*, 11, 1333-
764 1351, 2005.

765 Körner, M., Waser, B., Rehmann, R., and Reubi, J. C.: Early over-expression of GRP
766 receptors in prostatic carcinogenesis, *The Prostate*, 74, 217-224, 10.1002/pros.22743, 2014.

767 Law, R. M., Kowalczyk, E. A., and Wang, Y. P.: Using atmospheric CO₂ data to assess a
768 simplified carbon-climate simulation for the 20th century, *Tellus Ser. B-Chem. Phys.*
769 *Meteorol.*, 58, 427-437, 2006.

770 Maina, G. G., Brown, J. S., and Gersani, M.: Intra-plant versus inter-plant root competition in
771 beans: avoidance, resource matching or tragedy of the commons, *Plant Ecology*, 160, 235-
772 247, 2002.

773 Makela, A., Landsberg, J., Ek, A. R., Burk, T. E., Ter-Mikaelian, M., Agren, G. I., Oliver, C.
774 D., and Puttonen, P.: Process-based models for forest ecosystem management: current state of
775 the art and challenges for practical implementation, *Tree Physiol.*, 20, 289-298, 2000.

776 McConnaughay, K. D. M., and Bazzaz, F. A.: Is Physical Space a Soil Resource?, *Ecology*,
777 72, 94-103, 10.2307/1938905, 1991.

778 McMurtrie, R., and Wolf, L.: A model of competition between trees and grass for radiation,
779 water and nutrients, *Annals of Botany (London)*, 52, 449-458, 1983.

780 Medlyn, B. E., Duursma, R. A., Eamus, D., Ellsworth, D. S., Prentice, I. C., Barton, C. V. M.,
781 Crous, K. Y., de Angelis, P., Freeman, M., and Wingate, L.: Reconciling the optimal and
782 empirical approaches to modelling stomatal conductance, *Glob. Change Biol.*, 17, 2134-2144,
783 10.1111/j.1365-2486.2010.02375.x, 2011.

784 Metropolis, N., Rosenbluth, A. W., Rosenbluth, M. N., Teller, A. H., and Teller, E.: Equation
785 of State Calculations by Fast Computing Machines, *J. Chem. Phys.*, 21, 10.1063/1.1699114,
786 1953.

787 Mitchell, R. J., Liu, Y., O'Brien, J. J., Elliott, K. J., Starr, G., Miniati, C. F., and Hiers, J. K.:
788 Future climate and fire interactions in the southeastern region of the United States, *Forest*
789 *Ecology and Management*, 327, 316-326, <https://doi.org/10.1016/j.foreco.2013.12.003>, 2014.

790 Müller, C., Cramer, W., Hare, W. L., and Lotze-Campen, H.: Climate change risks for
791 African agriculture, *Proceedings of the National Academy of Sciences*, 108, 4313-4315,
792 10.1073/pnas.1015078108, 2011.

793 Nikinmaa, E., Sievänen, R., and Hölttä, T.: Dynamics of leaf gas exchange, xylem and
794 phloem transport, water potential and carbohydrate concentration in a realistic 3-D model tree
795 crown, *Annals of Botany*, 114, 653-666, [10.1093/aob/mcu068](https://doi.org/10.1093/aob/mcu068), 2014.

796 Paul, M. J., and Foyer, C. H.: Sink regulation of photosynthesis, *J Exp Bot*, 52, 1383-1400,
797 2001.

798 Pinnington, E. M., Casella, E., Dance, S. L., Lawless, A. S., Morison, J. I. L., Nichols, N. K.,
799 Wilkinson, M., and Quaife, T. L.: Investigating the role of prior and observation error
800 correlations in improving a model forecast of forest carbon balance using Four-dimensional
801 Variational data assimilation, *Agricultural and Forest Meteorology*, 228-229, 299-314,
802 <https://doi.org/10.1016/j.agrformet.2016.07.006>, 2016.

803 Poorter, H., Böhler, J., van Dusschoten, D., Climent, J., and Postma, J. A.: Pot size matters: a
804 meta-analysis of the effects of rooting volume on plant growth, *Funct Plant Biol*, 39, 839-
805 850, [10.1071/fp12049](https://doi.org/10.1071/fp12049), 2012a.

806 Poorter, H., Niklas, K. J., Reich, P. B., Oleksyn, J., Poot, P., and Mommer, L.: Biomass
807 allocation to leaves, stems and roots: meta-analyses of interspecific variation and
808 environmental control, *New Phytologist*, 193, 30-50, [10.1111/j.1469-8137.2011.03952.x](https://doi.org/10.1111/j.1469-8137.2011.03952.x),
809 2012b.

810 Pugh, T. A. M., Müller, C., Arneeth, A., Haverd, V., and Smith, B.: Key knowledge and data
811 gaps in modelling the influence of CO₂ concentration on the terrestrial carbon sink, *Journal*
812 *of Plant Physiology*, 203, 3-15, <https://doi.org/10.1016/j.jplph.2016.05.001>, 2016.

813 Quaife, T., Lewis, P., De Kauwe, M., Williams, M., Law, B. E., Disney, M., and Bowyer, P.:
814 Assimilating canopy reflectance data into an ecosystem model with an Ensemble Kalman
815 Filter, *Remote Sens. Environ.*, 112, 1347-1364, <https://doi.org/10.1016/j.rse.2007.05.020>,
816 2008.

817 Reich, P. B.: Key canopy traits drive forest productivity, *Proceedings of the Royal Society B:*
818 *Biological Sciences*, [10.1098/rspb.2011.2270](https://doi.org/10.1098/rspb.2011.2270), 2012.

819 Richardson, A. D., Williams, M., Hollinger, D. Y., Moore, D. J. P., Dail, D. B., Davidson, E.
820 A., Scott, N. A., Evans, R. S., Hughes, H., Lee, J. T., Rodrigues, C., and Savage, K.:
821 Estimating parameters of a forest ecosystem C model with measurements of stocks and fluxes
822 as joint constraints, *Oecol.*, 164, 25-40, 10.1007/s00442-010-1628-y, 2010.

823 Richardson, A. D., Carbone, M. S., Keenan, T. F., Czimczik, C. I., Hollinger, D. Y.,
824 Murakami, P., Schaberg, P. G., and Xu, X. M.: Seasonal dynamics and age of stemwood
825 nonstructural carbohydrates in temperate forest trees, *New Phytologist*, 197, 850-861,
826 10.1111/nph.12042, 2013.

827 Robbins, N. S., and Pharr, D. M.: Effect of Restricted Root Growth on Carbohydrate
828 Metabolism and Whole Plant Growth of *Cucumis sativus* L, *Plant Physiol.*, 87,
829 409-413, 10.1104/pp.87.2.409, 1988.

830 Rowland, L., Hill, T. C., Stahl, C., Siebicke, L., Burban, B., Zaragoza-Castells, J., Ponton, S.,
831 Bonal, D., Meir, P., and Williams, M.: Evidence for strong seasonality in the carbon storage
832 and carbon use efficiency of an Amazonian forest, *Glob. Change Biol.*, 20, 979-991,
833 10.1111/gcb.12375, 2014.

834 Running, S. W., and Gower, S. T.: FOREST-BGC, A general model of forest ecosystem
835 processes for regional applications. II. Dynamic carbon allocation and nitrogen budgets1,
836 *Tree Physiol.*, 9, 147-160, 10.1093/treephys/9.1-2.147, 1991.

837 Sage, R. F.: Acclimation of photosynthesis to increasing atmospheric CO₂: the gas-exchange
838 perspective, *Photosynthesis Research*, 39, 351-368, 1994.

839 Sala, A., Woodruff, D. R., and Meinzer, F. C.: Carbon dynamics in trees: feast or famine?,
840 *Tree Physiol.*, 32, 764-775, 10.1093/treephys/tpr143, 2012.

841 Schiestl-Aalto, P., Kulmala, L., Mäkinen, H., Nikinmaa, E., and Mäkelä, A.: CASSIA – a
842 dynamic model for predicting intra-annual sink demand and interannual growth variation in
843 Scots pine, *New Phytologist*, 206, 647-659, 10.1111/nph.13275, 2015.

844 Schwarz, G.: Estimating the Dimension of a Model, *Ann. Statist.*, 6, 461-464,
845 10.1214/aos/1176344136, 1978.

846 Thornley, J. H. M., and Cannell, M. G. R.: Modelling the Components of Plant Respiration:
847 Representation and Realism, *Annals of Botany*, 85, 55-67, 10.1006/anbo.1999.0997, 2000.

848 Thornton, P. E., Lamarque, J.-F., Rosenbloom, N. A., and Mahowald, N. M.: Influence of
849 carbon-nitrogen cycle coupling on land model response to CO₂ fertilization and climate
850 variability, *Global Biogeochemical Cycles*, 21, n/a-n/a, 10.1029/2006GB002868, 2007.

851 Van Oijen, M.: Bayesian Calibration (BC) and Bayesian Model Comparison (BMC) of
852 Process-Based Models: Theory, Implementation and Guidelines, 2008.

853 Villar, R., and Merino, J.: Comparison of leaf construction costs in woody species with
854 differing leaf life-spans in contrasting ecosystems, *New Phytologist*, 151, 213-226,
855 10.1046/j.1469-8137.2001.00147.x, 2001.

856 Wiley, E., and Helliker, B.: A re-evaluation of carbon storage in trees lends greater support
857 for carbon limitation to growth, *New Phytologist*, 195, 285-289, 10.1111/j.1469-
858 8137.2012.04180.x, 2012.

859 Williams, M., Schwarz, P. A., Law, B. E., Irvine, J., and Kurpius, M. R.: An improved
860 analysis of forest carbon dynamics using data assimilation, *Glob. Change Biol.*, 11, 89-105,
861 2005.

862 Zaehle, S., and Friend, A. D.: Carbon and nitrogen cycle dynamics in the O-CN land surface
863 model: 1. Model description, site-scale evaluation, and sensitivity to parameter estimates,
864 *Global Biogeochemical Cycles*, 24, n/a-n/a, 10.1029/2009GB003521, 2010.

865 Zobitz, J. M., Desai, A. R., Moore, D. J. P., and Chadwick, M. A.: A primer for data
866 assimilation with ecological models using Markov Chain Monte Carlo (MCMC), *Oecol.*, 167,
867 599, 10.1007/s00442-011-2107-9, 2011.

868

Inferring the effects of sink strength on plant carbon balance processes from experimental measurements

Kashif Mahmud¹, Belinda E. Medlyn¹, Remko A. Duursma¹, Courtney Campany^{1,2}, Martin G. De Kauwe³

Supplementary Information

Supplementary Section S1: Time dependent parameters

Supplementary Table S1: BIC values from time dependent parameter fit. The lowest BIC values indicate the best performing parameter setting. Treatment groups are: ‘Small’ - 5 L, 10 L and 15 L containers; ‘Large’ - 20 L, 25 L and 25 L containers; ‘Free’ – freely rooted seedlings.

Supplementary Figure S1: Total C mass in foliage NSC $C_{n,f}$ (lines) with **inferred parameter** settings and corresponding observations (symbols). Note that the NSC pool (y-axes) are plotted on log scale to visualize the changes at the beginning of the experiment. Error bars (1 SE, $n = 6$) are shown for each observation.

Supplementary Figure S2: Temporal evolution of carbon use efficiency (CUE) for various treatments.

Supplementary material

S1. Time dependent parameters

This section tests the time-dependency of CBM parameters (k , Y , a_f , a_w , a_r , s_f) due to ontogenetic or seasonal effects. We considered two alternative parameter sets to allow this variation from the default constant parameter setup with one set of parameters, p that does not change with time:

- a) Linear ($p = p_1 + p_2 * t$): Two sets of parameters representing linear variation over time,
- b) Quadratic ($p = p_1 + p_2 * t + p_3 * t^2$): Three sets of parameters that result in quadratic variation with time.

We examined whether parameters varied over time by comparing the BIC values for constant, linear, and quadratic parameter settings. The results are illustrated in Table S1 (Simulation Set D), which shows the effect of time dependency. Changing from constant to linear time-dependences improved BIC values for every treatment, indicating that there is significant variation over time in at least some parameters. Changing from linear to quadratic

variation in parameter values also improved the goodness of fit, although to a smaller but significant extent. For example, with the optimum treatment grouping option (3 groups), BIC values indicate that the quadratic variation over time in parameters is the best option; BIC numbers are reduced by around 16%, 2% and 20% for small container, large container and free seedlings respectively from linear to quadratic parameter settings (Table S1). We also tested 3rd degree polynomial equations for parameter variation (not shown), but it increased model complexity without improving the fit.

Supplementary Table S1: BIC values from time dependent parameter fit. The lowest BIC values indicate the best performing parameter setting. Treatment groups are: ‘Small’ - 5 L, 10 L and 15 L containers; ‘Large’ - 20 L, 25 L and 25 L containers; ‘Free’ – freely rooted seedlings.

Simulation set	Model settings	Treatment groups	BIC
D	Constant parameter variation	Small	1391
		Large	646
		free	332
	Linear parameter variation	Small	826
		Large	462
		free	217
	Quadratic parameter variation	Small	683
		Large	457
		free	170

